

## Accepted Manuscript

A novel biphenolic ligand for selective Mg<sup>2+</sup> and Zn<sup>2+</sup> ions sensing followed by colorimetric, spectroscopic and cell imaging methods

Palanisamy Uma Maheswari, Duraisamy Renuga, H.L. Jeeva Kumari, Kandasamy Ruckmani



PII: S0928-0987(18)30032-0  
DOI: <https://doi.org/10.1016/j.ejps.2018.01.025>  
Reference: PHASCI 4375

To appear in: *European Journal of Pharmaceutical Sciences*

Received date: 30 April 2017  
Revised date: 20 December 2017  
Accepted date: 11 January 2018

Please cite this article as: Palanisamy Uma Maheswari, Duraisamy Renuga, H.L. Jeeva Kumari, Kandasamy Ruckmani, A novel biphenolic ligand for selective Mg<sup>2+</sup> and Zn<sup>2+</sup> ions sensing followed by colorimetric, spectroscopic and cell imaging methods. The address for the corresponding author was captured as affiliation for all authors. Please check if appropriate. Phasci(2017), <https://doi.org/10.1016/j.ejps.2018.01.025>

This is a PDF file of an unedited manuscript that has been accepted for publication. As a service to our customers we are providing this early version of the manuscript. The manuscript will undergo copyediting, typesetting, and review of the resulting proof before it is published in its final form. Please note that during the production process errors may be discovered which could affect the content, and all legal disclaimers that apply to the journal pertain.

Submitted to: *Eur.J. Pharm. Sci.* 2017

Article type: Full Paper

**A novel biphenolic ligand for selective Mg<sup>2+</sup> and Zn<sup>2+</sup> ions sensing followed by colorimetric, spectroscopic and cell imaging methods.**

Palanisamy Uma Maheswari,<sup>a\*</sup> Duraisamy Renuga,<sup>b</sup> H.L.Jeeva Kumari<sup>c</sup> and Kandasamy Ruckmani<sup>c\*</sup>

<sup>a</sup> Department of Chemistry, National Institute of Technology, Tiruchirappalli – 620015, Tamilnadu, India.

<sup>b</sup> Department of Chemistry, Selvamm College of Technology, Namakkal – 637003, Tamilnadu, India.

<sup>c</sup> Department of Pharmaceutical Technology, Centre for Excellence in Nanobio Translational Research (CENTRE), Bharathidasan Institute of Technology, Anna University, Tiruchirappalli 620024, Tamil Nadu, India

Key words: MgCl<sub>2</sub>, ZnCl<sub>2</sub>, colorimetric, fluorescence microscopy, live cell imaging.

## 1. Introduction

The design and synthesis of chemo sensors for biologically important metal ions have emerged as the most important topic in the field of medicinal chemistry and live cell imaging. (Kyle et al. 2014). The chemo sensors are expected to be selective, easy to prepare, with good ADME profile, low cytotoxicity during the imaging duration and good association constant on binding to the metal ions (Lok Nath et al., 2016). The chemo sensors are widely used for calorimetric, fluorometric detection of metal ions, which can be observed by naked eye, fluorescence spectrophotometer or by a fluorescence microscopy. The chemo sensors have been extrapolated with intracellular or extracellular applications for various metal ions, whether they are present in trace or bulk concentrations (Yifan et al., 2016). The sensor absorption and emission profile should be appreciable especially after binding to metal ions with good quantum yield. The intense emissive property of the chemo sensors on binding to metal ions are widely used in live cell imaging of biologically important metal ions to follow the metabolism often. The chemo sensors are usually designed by appropriate coordination sites suitable for the detection of the respective metal ions based on their size and appending a fluorophore to the designed receptor for fluorometric detection *in-vitro* and *in-vivo* (Lourdes et al., 2007). This method is advantageous over atomic absorption spectroscopy, ion-selective electrodes etc as this can be applicable to living cell and physiological conditions. The chemo sensors have been used to detect Hg, Pb, Mg, Ca, Cu, Zn and many other metal ions through live cell imaging (Yong Sung et al., 2016; Kim et al., 2014; Tayade et al., 2014; Tayade et al., 2014; Liu et al., 2012).

Magnesium ions has major role in the biological systems and considered as an important factor participating in many biochemical reactions, cell growth, in stabilizing the double stranded DNA conformation and even in regulating the calcium ion channels (Cowan et al., 2002).  $Mg^{2+}$  is also present in chlorophyll and involved in photosynthesis of carbohydrates.  $Mg^{2+}$  is a bulk metal in need for muscle coordination and bone health, for functioning of nerves and immune systems and reason for many congestive cardiac diseases (Wolf et al., 2003). The concentration of  $Mg^{2+}$  ions in cells vary from 1 mM to 6 mM. Thus,  $Mg^{2+}$  estimation *in-vivo* can be an important tool to follow the function or dysfunction of human body, appropriately. The sample can be as simple as the blood serum for detection. Zinc metal ions also has role in muscle strengthening, as a co- factor in many hydroxylation enzymes, part of zinc fingers and help towards many bio-transformations and signaling (Li et al., 2014; Zhipeng et al., 2014).

Detection of both  $\text{Mg}^{2+}$  and  $\text{Zn}^{2+}$  separately and together by a chemo sensor can be an important application. The biphenolic receptor prepared from salicylaldehyde and 2-amino-4-methyl phenol found to detect  $\text{Mg}^{2+}$  and  $\text{Zn}^{2+}$  selectively and has no specificity for other metal ions (Scheme 1). The paper describes the calorimetric, absorption and emission spectroscopic detection of Mg and Zn ions by the receptor and its live cell imaging of the same metal ions, *in vitro*.

## 2. Materials and Methods

### 2.1. Materials

The chemicals and solvents were all of analytical grade were used without further purification. Salicylaldehyde, 2-amino 4-methyl phenol and metal salts were purchased from Sigma-Aldrich, Bangalore and used as such. HeLa cells were obtained from National Centre for Cell Science (NCCS), Pune, India. Dulbecco's modified Eagle's medium (DMEM) and fetal bovine serum (FBS) were procured from Invitrogen, USA. 3-(4,5-dimethylthiazol-2-yl)-2,5-diphenyltetrazolium bromide (MTT) was purchased from Hi media, Mumbai, India. Milli Q water was used to prepare solutions and buffers.

### 2.2. Methods

IR spectra were obtained on a Perkin-Elmer spectrophotometer.  $^1\text{H}$  and  $^{13}\text{C}$  NMR spectra were recorded on a Bruker 400 MHz spectrometer with  $\text{DMSO-d}_6$  as solvent. Varian spectrophotometer was used to record absorption and fluorescence emission spectra. For calorimetric, absorption and emission titration, a stock solution of the  $\text{ZnCl}_2$  or  $\text{MgCl}_2$  ( $1.5 \times 10^{-3}\text{M}$ ) was prepared in pure water. The receptor solution ( $5 \times 10^{-5}\text{M}$ ) was prepared in DMSO. For each titration, 3 ml of receptor was titrated with 0.1 eq (10  $\mu\text{L}$ ) – 1 eq (100  $\mu\text{L}$ ) of the respective  $\text{Zn}^{2+}$  or  $\text{Mg}^{2+}$  ions in DMSO/water medium. For cyclic voltammetric studies, EG and G potentiostat was used. The receptor solution was prepared in 1 mM concentration for about 20 mL of volume with  $\text{CH}_3\text{CN}$  as solvent. The supporting electrolyte was tetrabutylammonium hexafluorophosphate. The respective metal ions were added in 2 equivalents to the receptor concentration to follow the metal ion detection. Platinum plate and platinum wire were used as a working and counter electrode.  $\text{Ag}^+/\text{Ag}$  was used as the reference electrode.

### 2.3. Synthesis of the receptor

The receptor was prepared by a simple condensation method. Salicylaldehyde (5 mmol, 0.6106 g) was dissolved in 20 mL of warm ethanol and 2-amino-4-methyl phenol (5 mmol, 0.6157g) was added to the ethanol solution dropwise. The mixture was slowly kept under reflux for 6 h at 75°C. On cooling, a red brown coloured solid separated out, which was filtered and washed with ethanol and then dried in vacuum. Yield was 0.9787g (84%). The structure of the receptor was confirmed by NMR spectroscopy. <sup>1</sup>H NMR (400MHz, DMSO-d<sub>6</sub>): δ 3.3 (1H, s), δ 6.8 – δ 7.6 (4H, m), δ 8.9 (1H, s), δ 9.5 (1H, s), δ 13.8 (1H, s).; <sup>13</sup>C NMR (100MHz, DMSO-d<sub>6</sub>): δ 21.0, δ 117.2, δ 117.5, δ 119.6, δ 120.4, δ 120.7, δ129.2, δ 133.1, δ133.6, δ135.3. CHN analysis for the formula C<sub>14</sub>H<sub>13</sub>N<sub>1</sub>O<sub>2</sub>. Found (calculated); C; 73.56 (73.99%); H; 5.40 (5.77%); N; 6.02 (6.16%).

### 2.4. Cytotoxicity studies

HeLa cancer cells were maintained at 1 x 10<sup>6</sup> cells/mL in DMEM, supplemented with 10% heat-inactivated FBS and incubated at 37 °C in an atmosphere with 5% CO<sub>2</sub>. Cells were maintained in a 96-well plate at a density of 2 x 10<sup>4</sup> cells/well and kept to attach over the night. The medium was discarded and the cells were incubated with different concentrations (6.25-200 μM) of the receptor sample for 24 h. The sample was dissolved in dimethyl sulfoxide (DMSO) at a stock concentration of 32 mM. The final concentration of DMSO was not exceeded 0.625 % for every treatment, and it was used as a negative control. The assays were performed in triplicate (Sudeshna et al., 2008). MTT dye reduction assay was performed to determine the percentage of cell viability and the anticancer effect of sample at various concentrations. The assay depends on the reduction of MTT by mitochondrial dehydrogenase, an enzyme present in the mitochondria of viable cells to a purple coloured formazan product. After 24 h incubation at 37 °C in 5% CO<sub>2</sub> atmosphere, the cells were washed with phosphate-buffered saline (PBS). The morphology of the cells was observed under an inverted microscope and the phase-contrast images were acquired at 20 X magnification. 20 μL of MTT (5 mg /mL) was then added and incubated for 4 h. The medium was discarded and 100 μL of DMSO was added to dissolve the formazan crystals. The absorbance was read at 570 nm in a microplate reader. The percentage of cell viability and the percentage of inhibition at various concentrations were calculated using the following formulae:

$$\% \text{ viability} = (A_t / A_c) \times 100 \dots\dots\dots(1)$$

$$\% \text{ inhibition} = (A_c - A_t) / A_c \times 100 \dots\dots\dots(2)$$

where,  $A_t$  is the absorbance of the test sample and  $A_c$  is the absorbance of the control.

A graph was plotted between the concentration of the sample and percentage of inhibition, thereby determining the  $IC_{50}$  value of sample which is the maximal concentration of the drug to cause 50 % inhibition of biological activity of cancer cells.

### 2.5. Live-cell imaging studies

HeLa cells were seeded in a 24-well plate in DMEM at a density of  $3 \times 10^5$  cells/well incubated at  $37^\circ\text{C}$  at 5%  $\text{CO}_2$ . After an overnight incubation, the medium was discarded and the cells were incubated with different concentrations (6.25 - 200  $\mu\text{M}$ ) of receptor for 30 min at  $37^\circ\text{C}$ . The cells were washed thrice with PBS and observed under an inverted fluorescence microscope for a control. The receptor concentration was varied as 6.25, 12.5, 25, 50, 100 and 200  $\mu\text{M}$  concentrations for each set of experiment. After acquiring the images of HeLa cells incubated with varying concentrations of receptor for 30 min, addition of individual metal ions ( $\text{Mg}^{2+}$ ,  $\text{Zn}^{2+}$ ,  $\text{Ca}^{2+}$ ) to each set of experiment with mentioned concentrations were performed simultaneously and also one set was a mixture of  $\text{Mg}^{2+}$  and  $\text{Zn}^{2+}$  ions. The bright field and fluorescence images were acquired at 20 X magnification for each set of experiment (Udhayakumari et al., 2014). The mean fluorescence intensities of treated samples with individual metal ions ( $\text{Mg}^{2+}$ ,  $\text{Zn}^{2+}$ ,  $\text{Ca}^{2+}$ ) and combination ( $\text{Mg}^{2+}$  and  $\text{Zn}^{2+}$ ) were compared using NIS-Elements D software (version 4.13), Ti-E, Nikon, Japan, and a graph was plotted with concentration of the sample vs. fluorescence intensity for evaluation.

## 3. Results and Discussion

### 3.1. Colorimetric titrations

The sensing property of the receptor towards various cations was studied by calorimetric method. In the calorimetric experiments, 3 mL of receptor solution in DMSO/ $\text{H}_2\text{O}$  ( $5 \times 10^{-5}$  M) was titrated with the respective metal ion solutions in  $\text{H}_2\text{O}$  medium. With 1 equivalents of  $\text{ZnCl}_2$  or  $\text{MgCl}_2$  ( $1.5 \times 10^{-3}$  M) the color change was observed. The color changes are as shown in the Figs. 1 and 2. The receptor solution changed to bright yellow from colorless solution for  $\text{Zn}^{2+}$ , immediately. The  $\text{Mg}^{2+}$  ions on interaction with the receptor produce yellow color change, after

30 minutes. Other cations like  $K^+$ ,  $Na^{2+}$  and  $Ca^{2+}$  (up to 10 equivalents), transition metal ions like  $Cr^{2+}$ ,  $Fe^{2+}$ ,  $Ni^{2+}$ ,  $Co^{2+}$ ,  $Cu^{2+}$  and heavy metal ions like  $Sn^{2+}$ ,  $Pd^{2+}$ ,  $Ce^{2+}$ ,  $Hg^{2+}$ ,  $Cd^{2+}$  do not show any color changes on interaction with the receptor.

### 3.2. UV-Visible spectroscopic studies

The sensing behavior of the receptor towards  $Zn^{2+}$  and  $Mg^{2+}$  ions were also followed by UV-Visible spectroscopy. The titration involves 1 mL of the receptor solution ( $5 \times 10^{-5}$  M) and incremental addition of respective metal ions upto 2 eq ( $1 \times 10^{-3}$  M) in DMSO/ $H_2O$  medium. The pure receptor in DMSO/ $H_2O$  medium showed a prominent absorption band at 360 nm. This band on  $Zn^{2+}$  coordination decreases in intensity and a new band at 450 nm found to be increasing in intensity. The 360 nm band was assigned to  $\pi$  to  $\pi^*$  transition and the new band at 450 nm was assigned to metal to ligand charge transfer band. The observation of two isosbestic points clearly depicted a single binding event (Fig. 3). A similar trend was also observed for  $Mg^{2+}$  ions binding to the receptor (Fig. 4). Both  $Zn^{2+}$  and  $Mg^{2+}$  ions showed 8 to 10 fold increase in the new band intensity. This ensures the same binding mode for both metal ions to the receptor. The investigation of absorption spectral changes of the receptor upon addition of various other metal ions with the same concentrations or even at higher concentrations showed no prominent spectral changes (Fig. 5). It reveals the selective binding of the receptor to  $Zn^{2+}$  and  $Mg^{2+}$  ions only and not to any other metal ions. Therefore, it was clear that the receptor can be used for selective sensing of  $Zn^{2+}$  and  $Mg^{2+}$  over a wide range of cations.

### 3.3. Fluorescence spectroscopic studies

The receptor binding to  $Zn^{2+}$  and  $Mg^{2+}$  ions binding was also followed by emission spectra. Titration experiments were carried out similar to absorption spectroscopy with the same concentrations and volume. When the pure receptor is excited at 450 nm, it gave a very weak emission band around 525 nm but after the addition to  $Zn^{2+}$  ions, it gave a strong emission band at 560 nm with a red shift (Fig 6). The same titration of the receptor with  $Mg^{2+}$  ions, showed similar emission trend but with 100 and above fold of increase in emission intensity at the band around 560 nm (Fig. 7). The  $K$  (binding constant) values are determined using scatchard plots and fluorescence data and were found to be  $4.28 \pm 0.62$  for  $Zn^{2+}$ ; and  $15.14 \pm 0.24$  for  $Mg^{2+}$ . The many fold increase in emission intensity on binding of  $Mg^{2+}$  ions compared to  $Zn^{2+}$  ions shows

the facile binding event and the much increase in fluorescence emission. As observed in the absorption spectroscopy, the emission increase was selectively observed only in the case of  $\text{Zn}^{2+}$  and  $\text{Mg}^{2+}$  ions and other metal ions did not show any prominent increase in the emission intensity (Fig. 8).

### 3.4. Job's plot studies

The Job's plot study was done as described elsewhere (Renuga et al., 2012), with the receptor and the  $\text{Zn}^{2+}$  or  $\text{Mg}^{2+}$  ions, with the concentration fixed at  $5 \times 10^{-3} \text{M}$  in DMSO/ $\text{H}_2\text{O}$  medium (Fig 9). The volume of the solution was 3 mL and kept constant through out the study. Absorption at 450 nm was chosen for the observation. The studies revealed the binding stoichiometry as 2:1 for receptor:  $\text{Zn}^{2+}$  or  $\text{Mg}^{2+}$  ions as shown in the Scheme 2.

### 3.5. Binding sites of the receptor to $\text{Zn}^{2+}$ or $\text{Mg}^{2+}$ ions probed by $^1\text{H}$ NMR

The pure receptor, in DMSO- $\text{d}_6$  showed the two phenolic protons at  $\delta 8.9$  (Fig. 10, 1) and  $9.5$  (Fig. 10, 2). On binding to  $\text{Zn}^{2+}$  or  $\text{Mg}^{2+}$  ions these two protons are highly perturbed than the imine proton at  $\delta 13.7$  (Fig. 10, 3). After addition of 1 equivalent of  $\text{Zn}^{2+}$  or  $\text{Mg}^{2+}$  ions, the phenolic protons are completely deprotonated and the binding occurs through the two 'O' donors as revealed by the NMR spectroscopy. But the imine proton exchange due to the coordination of the receptor became medium rather than fast or slow for intermolecular interactions, so the respective NMR peak also became less intense.

### 3.6. Cyclic voltammetry studies

The cyclic voltammogram of the pure receptor showed an oxidation peak at around  $0.7 \text{ V}$  (Fig 11). The scan speed was  $100 \text{ mV/s}$  and the voltammogram was an average presentation of five scans. The potential window was kept from  $-1$  to  $+1 \text{ V}$ . The oxidation peak was assigned to be phenol to phenoxyl radical formation under applied potential. This oxidation peak which corresponds to phenoxyl radical formation generally on coordination occurs at less potential than the pure receptor. Thus on addition of 1 equivalent of  $\text{ZnCl}_2$  the oxidation occurred at  $0.68 \text{ V}$  and the same oxidation occurs at  $0.5 \text{ V}$  on addition of 1 equivalent of  $\text{MgCl}_2$  (Fig. 12). The oxidation

peak thus reveals the facile coordination of the two phenolates of the receptor to  $Mg^{2+}$  rather than  $Zn^{2+}$  ions.

### 3.7. Cytotoxicity assay

The morphological assessment of the cells (Fig. 13) reveals that the treatment of receptor at dose dependent concentration on HeLa cells reduced the cell viability by altering cellular morphology. The morphological characteristics include shrinkage of cells, reduced cell density, reduction in cell to cell contact when compared to that of untreated cells (control). Increase in the concentration of receptor indicates the cytotoxic effect of receptor on HeLa cancer cells. Negative control did not show any cytotoxicity similar to untreated (control) cells, hence it was considered negligible. The cytotoxic effect of the receptor is found to increase with increase in concentration, resulting in a direct dose-response relationship. A maximum of 93.28% inhibition is observed at 200  $\mu M$  at 24 hours of incubation time and the  $IC_{50}$  value is found to be 80.74  $\mu M$  (equivalent to 18.16  $\mu g/mL$ ) (Fig. 14).

### 3.8. Live cell imaging studies

The phase contrast and fluorescence images of HeLa cells were captured after being incubated with receptor, receptor +  $Mg^{2+}$  (Fig. 15), receptor +  $Zn^{2+}$  (Fig. 16) and receptor +  $Mg^{2+}$  +  $Zn^{2+}$  (Fig. 17) for 30 min at 37°C. The receptor alone, at the highest concentration of 200  $\mu M$ , on HeLa cells displayed least or no intracellular fluorescence. However, cells exhibited intense fluorescence on additional treatment with added  $Mg^{2+}$  and  $Zn^{2+}$  separately. Also the cells exhibited intense fluorescence with the mixture of  $Mg^{2+}$  and  $Zn^{2+}$ . These results clearly explain the intracellular detection of  $Zn^{2+}$  and  $Mg^{2+}$  ions and together by the biphenolic receptor. The minimum detection level was 12.5  $\mu M$  for  $Mg^{2+}$  and 25  $\mu M$  for  $Zn^{2+}$  ions. Like any other Mg sensors, which competitively detect  $Ca^{2+}$  ions also, the receptor is checked for the competitive sensing of  $Ca^{2+}$ . But as reflected in the absorption and emission studies,  $Ca^{2+}$  was not detected by the receptor, which makes this receptor to be very unique for  $Mg^{2+}$  sensing, even in the presence of bulk metal ions like  $Na^+$ ,  $K^+$ ,  $Ca^{2+}$  etc (Fig.18). The  $Zn^{2+}$  concentration inside the cells will be in nanomolar range which will not be the bulk species available for detection in comparison to  $Mg^{2+}$ . Thus this receptor have the ability to perform dual roles, as a sensor of both  $Mg^{2+}$  and  $Zn^{2+}$  ions, either singly or simultaneously; and may found application in biological

monitoring of these metal ions, selectively, because of its relatively low cytotoxicity up to 12 h, at the indicated dose and time of incubation.

### 3.9. Discussion

Generally the alkali and alkaline earth metals bind to soft donors like 'O' based ligands like crown ethers rather than hard, 'N' based ligands like histidine etc. In transition metal ions also Zn binds to 'O' based ligands like carboxylic acids etc. The biphenolic receptor used for the current study is thus a simple ligand with phenolic 'O' donors, binding to both  $Mg^{2+}$  and  $Zn^{2+}$  in 2:1 ratio, as compatible to the size of metal ions, namely  $Mg^{2+}$  and  $Zn^{2+}$ . The colorimetric change gives yellow color on metal ions binding to the receptor, a complimentary to the absorbed violet color. The yellow color of observance on the metal ions binding clearly indicates the facile n to  $\pi^*$  electronic transition stimulated in the receptor. The increase in the absorption band between 350 to 450 nm on the metal ions binding event clearly depicts the respective electronic transition. The unfavorable detection for other metal ions may be due to intermediate binding stoichiometry or the less symmetric coordination geometry or the less stability constants for the complex formed. The phenolic 'O' donor participation towards coordination of  $Mg^{2+}$  and  $Zn^{2+}$  comes from the cyclic voltammetry studies which shows the facile nature of the phenolate ligand on oxidation. The binding constants reveal the high binding affinity of the receptor for  $Mg^{2+}$  rather than  $Zn^{2+}$  metal ions. The cytotoxicity studies with HeLa cells reveal the dose dependent anticancer effect of the receptor at 24 hours of incubation. HeLa cells were chosen for cytotoxicity and live cell imaging studies as it is widely appreciated for fluorescence microscopy studies. The live cell imaging studies at half an hour incubation clearly depicts the sensing of the metal ions from the low concentrations of 12.5  $\mu M$  and 25  $\mu M$  for  $Mg^{2+}$  and  $Zn^{2+}$  ions, respectively. This concentration can be extended to the biological macro or micro nutrients concentration with a high definition microscopy which can observe the metal ions in the sub cellular organelles also. Thus the biphenolic receptor which gets stimulated with a high intensity n to  $\pi^*$  electronic transition responsible for the enhanced fluorescence with the microscopy observation can be good choice for the ultimate detection of  $Mg^{2+}$  or  $Zn^{2+}$  ions.

#### 4. Conclusion

The receptor was easily synthesized by simple condensation method of salicylaldehyde and 2-amino-4-methyl phenol. The structure of the receptor was confirmed by CHN, FT-IR,  $^1\text{H}$  NMR and  $^{13}\text{C}$  NMR spectroscopic techniques. This receptor is highly selective and sensitive towards Zn and Mg ions detection through calorimetric response. The binding of the metal ions changes the colorless solution of the receptor to bright turmeric yellow. Jobs plot studies reveal the stoichiometry of the complex formed between the receptor and the  $\text{Zn}^{2+}$  or  $\text{Mg}^{2+}$  ions as 2:1. The sensing property of the receptor was also probed by absorption and emission spectroscopy. In absorption spectroscopy, the pure receptor band at 360 nm decreases in intensity and a new band at 450 nm was observed with increase in intensity for both  $\text{Zn}^{2+}$  and  $\text{Mg}^{2+}$  ions binding. In emission spectroscopy, on excitation at 450 nm, both metal ions on binding showed enhancement in emission intensity with a band around 560 nm.  $\text{Mg}^{2+}$  ions showed 100 fold increase in emission intensity than  $\text{Zn}^{2+}$  ions which depicts the facile sensing and coordination of the  $\text{Mg}^{2+}$  ions in comparison with  $\text{Zn}^{2+}$  ions. This property is applied for live cell imaging of the Mg or Zn ions, using HeLa cells, *in-vitro*. The receptor showed cytotoxicity over 24 hours and less cytotoxic with in 12 hours. The live cell imaging was done by incubating the receptor with or without Mg or Zn ions for 30 minutes and were detected through fluorescence microscopy. The minimum detection level was 12.5  $\mu\text{M}$  for  $\text{Mg}^{2+}$  and 25  $\mu\text{M}$  for  $\text{Zn}^{2+}$  ions. Thus the receptor is highly useful for detecting the Mg and Zn ions, separately or together, without any other metal ions interference, through fluorescence microscopic techniques.

#### Acknowledgement

Dr. P. U. Maheswari acknowledges DST-SERB for financial support (project: SR/FT/CS-01/2011(G))

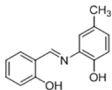
#### References

- Cowan, J.A.; et al.; 2002. Structural and catalytic chemistry of magnesium-dependent enzymes. *Biometals*.15(3), 225-235.
- Kim, KB.; et al., 2014. A fluorescent and colorimetric chemosensor for selective detection of aluminum in aqueous solution. *Tetrahedron Lett.* 55, 1347–1352.

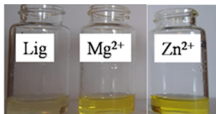
- Kyle, P., et al.; 2014. Fluorescent sensors for measuring metal ions in living systems. *Chem. Rev.* 114 (8), 4564–4601.
- Li, P.; et al.; 2014. A highly fluorescent chemosensor for Zn(2+) and the recognition research on distinguishing Zn(2+) from Cd(2+). *Dalton Trans.* 43, 706-714.
- Liu, Z.; et al., 2012. An excitation ratiometric Zn<sup>2+</sup> sensor with mitochondria-target ability for monitoring of mitochondrial Zn<sup>2+</sup> release upon different stimulations. *Chem Commun.* 48, 8365–8367.
- Lok Nath, N., et al., 2016. Selective and sensitive detection of heavy metal ions in 100% aqueous solution and cells with a fluorescence chemosensor based on peptide using aggregation-induced emission. *Anal. Chem.* 88 (6), 3333–3340.
- Lourdes, B., et al., 2007. Design of fluorescent materials for chemical sensing. *Chem. Soc. Rev.* 36, 993–1017.
- Renuga, D.; et al.; 2014. Novel thiophene based colorimetric and fluorescent receptor for selective recognition of fluoride ions. *Tetrahedron Letts.* 53, 5068-5070.
- Sudeshna, R.; et al.; 2008. Phenanthroline derivatives with improved selectivity as DNA targeting anticancer or antimicrobial drugs. *Chemmedchem.* 3(9), 1427–1434.
- Tayade, K.; et al., 2014. A fluorescent “turn-on” sensor for the biologically active Zn<sup>2+</sup> ion. *Inorg. Chim. Acta* 421, 538–543.
- Tayade, K.; et al., 2014. 2, 2-[benzene-1, 2-diylbis(iminomethanediyl)]diphenol derivative bearing two amine and hydroxyl groups as fluorescent receptor for zinc (II) ion. *Spectrochim Acta A* 126, 312–316.
- Udhayakumari, D.; et al.; 2014. Highly fluorescent probe for copper(II) ion based on commercially available compounds and live cell imaging. *Sens. Actuator B-Chem.* 198, 285-293.
- Wolf, F.I.; et al.; 2003. Cell physiology of magnesium. *Mol aspects Med.* 24(1-3), 11-26.
- Yifan, L., et al., 2016. Fluorescent and colorimetric chemosensors for anions, metal ions, reactive oxygen species, biothiols, and gases. *Bull. Korean Chem. Soc.* 37(10), 1661 -1678.
- Yong Sung, K.; et al., 2016. A turn-on fluorescent chemosensor for Zn<sup>2+</sup> Based on quinoline in aqueous media. *J. Fluoresc.* 26 (3), 835-844.
- Zhipeng, L.; et al.; 2014. In vivo ratiometric Zn<sup>2+</sup> imaging in zebrafish larvae using a new visible light excitable fluorescent sensor. *Chem. Commun.* 50, 1253-1255.

**Abstract**

The (E)-2-((2-hydroxy-5-methylphenylimino) methyl) phenol ligand was synthesized. The receptor was characterised by IR,  $^1\text{H}$  and  $^{13}\text{C}$  NMR and CHN analysis. The ligand exhibits colorimetric and fluorometric sensing of  $\text{Zn}^{2+}$  and  $\text{Mg}^{2+}$  ions in semi-aqueous medium (DMSO- $\text{H}_2\text{O}$ ). The receptor was tested with series of transition metal ions ( $\text{Cr}^{2+}$ ,  $\text{Fe}^{2+}$ ,  $\text{Ni}^{2+}$ ,  $\text{Co}^{2+}$ ,  $\text{Cu}^{2+}$ ,  $\text{Zn}^{2+}$ ) and heavy metal ions ( $\text{Sn}^{2+}$ ,  $\text{Pd}^{2+}$ ,  $\text{Ce}^{2+}$ ,  $\text{Hg}^{2+}$ ,  $\text{Cd}^{2+}$ ) and the essential human body elements like  $\text{Ca}^{2+}$ ,  $\text{Mg}^{2+}$ ,  $\text{Na}^+$  and  $\text{K}^+$  ions. The naked eye colorimetric sensing was absorbed only for  $\text{Zn}^{2+}$  and  $\text{Mg}^{2+}$ . Both ions ( $\text{ZnCl}_2$  and  $\text{MgCl}_2$  in  $\text{H}_2\text{O}$ ), when added to the colorless solutions of the receptor of about 1 equivalence in incremental additions turn the solution into bright turmeric yellow. All other ions remain inactive, in colorimetric sensing. Further the  $\text{Zn}^{2+}$  and  $\text{Mg}^{2+}$  ions were probed by absorption and emission spectroscopy through incremental addition of respective metal ions. The *in-situ* deprotonation of the ligand on both  $\text{Mg}^{2+}$  and  $\text{Zn}^{2+}$  ions binding was confirmed by  $^1\text{H}$  NMR titration studies. The imino nitrogen of the receptor is not coordinated to the metal ions. The Job's plot studies reveal the 1: 2 binding ratio of metal ions to the receptor. The high fold fluorescence output on metal ions binding was positively used to sense the  $\text{Zn}^{2+}$  and  $\text{Mg}^{2+}$  ions, separately and together in HeLa cancer cells through cell imaging.



Receptor

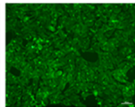
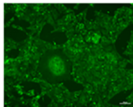


Calorimetric sensing of  $Mg^{2+}$  and  $Zn^{2+}$  ions

Receptor 1

Receptor 1 +  
 $100\mu M$  of  
 $Mg^{2+}$  &  $Zn^{2+}$

Receptor 1 +  
 $200\mu M$  of  
 $Mg^{2+}$  &  $Zn^{2+}$



Live cell imaging of  $Mg^{2+}$  and  $Zn^{2+}$  ions

Graphics Abstract

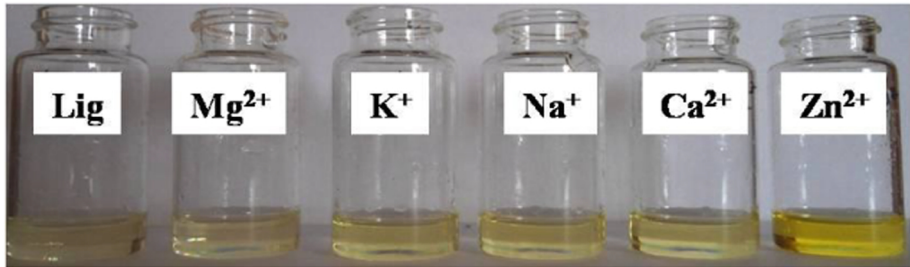


Figure 1

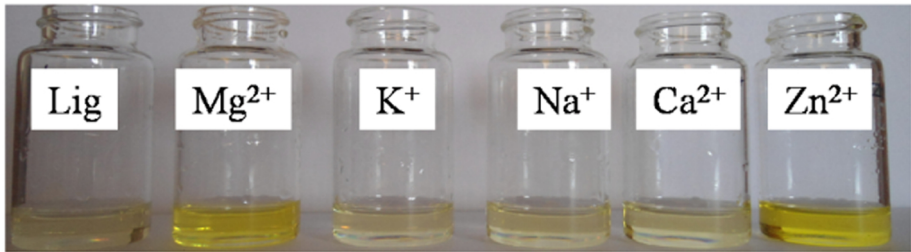


Figure 2

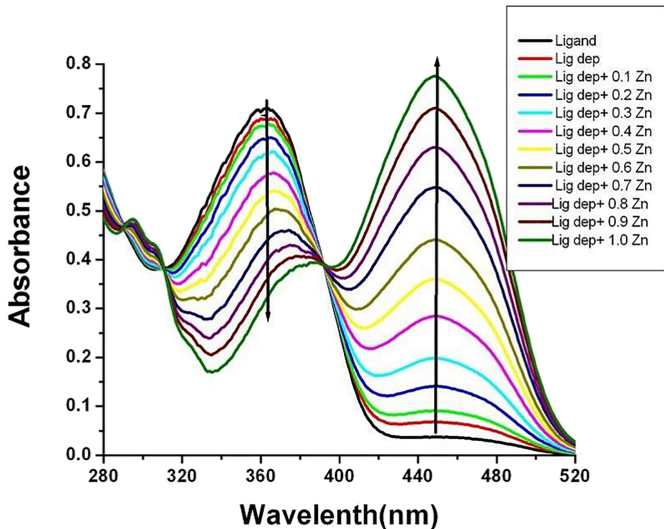


Figure 3

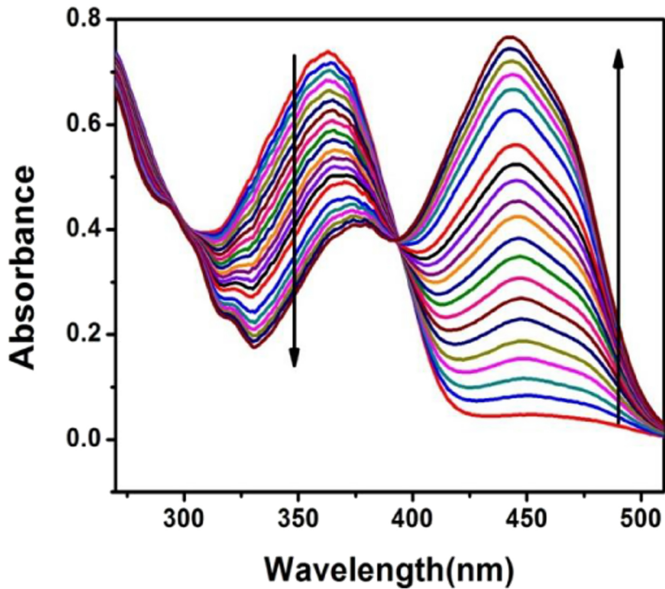


Figure 4

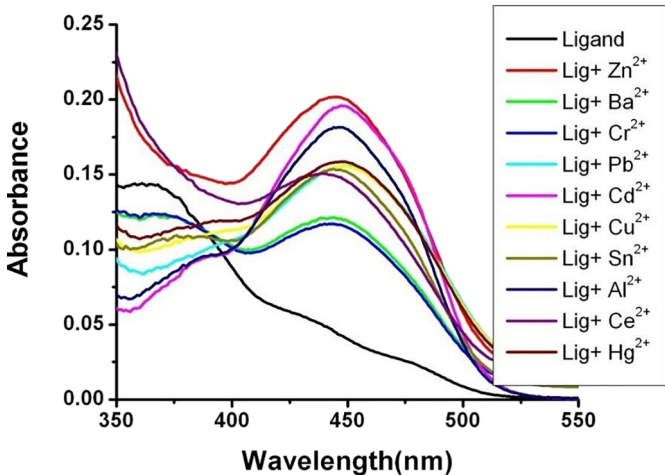


Figure 5

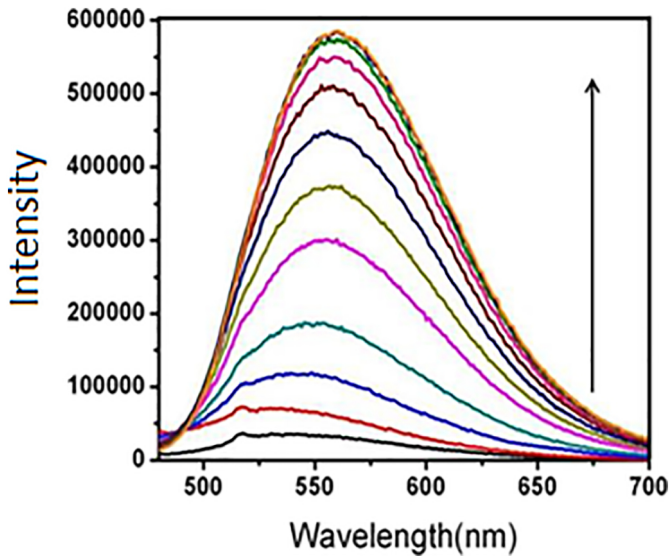


Figure 6

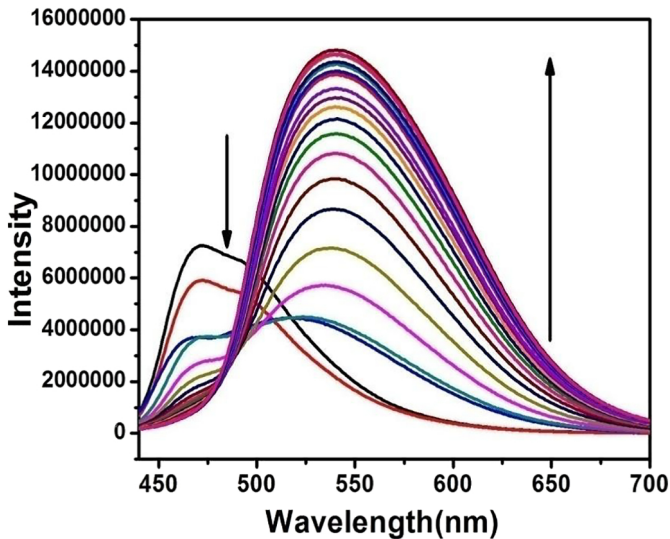


Figure 7

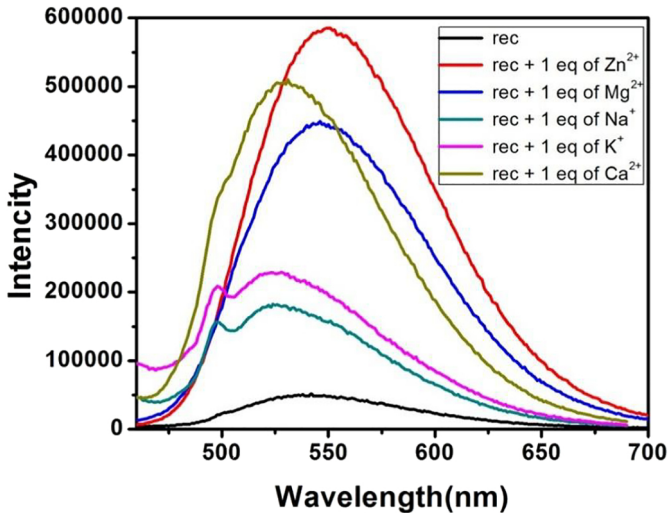


Figure 8

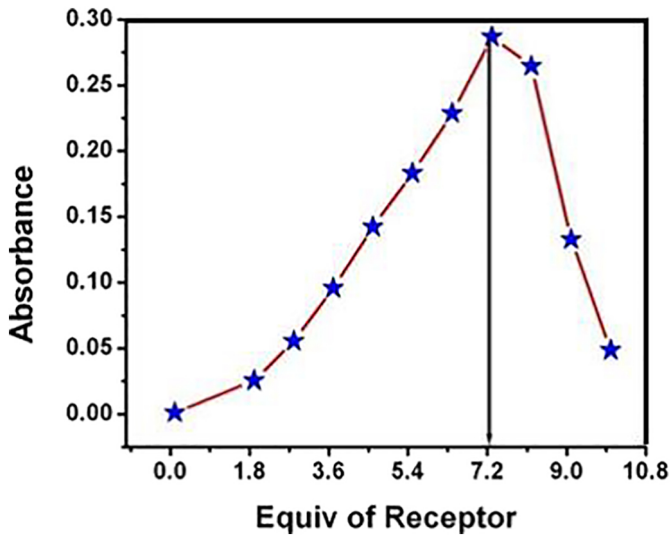


Figure 9

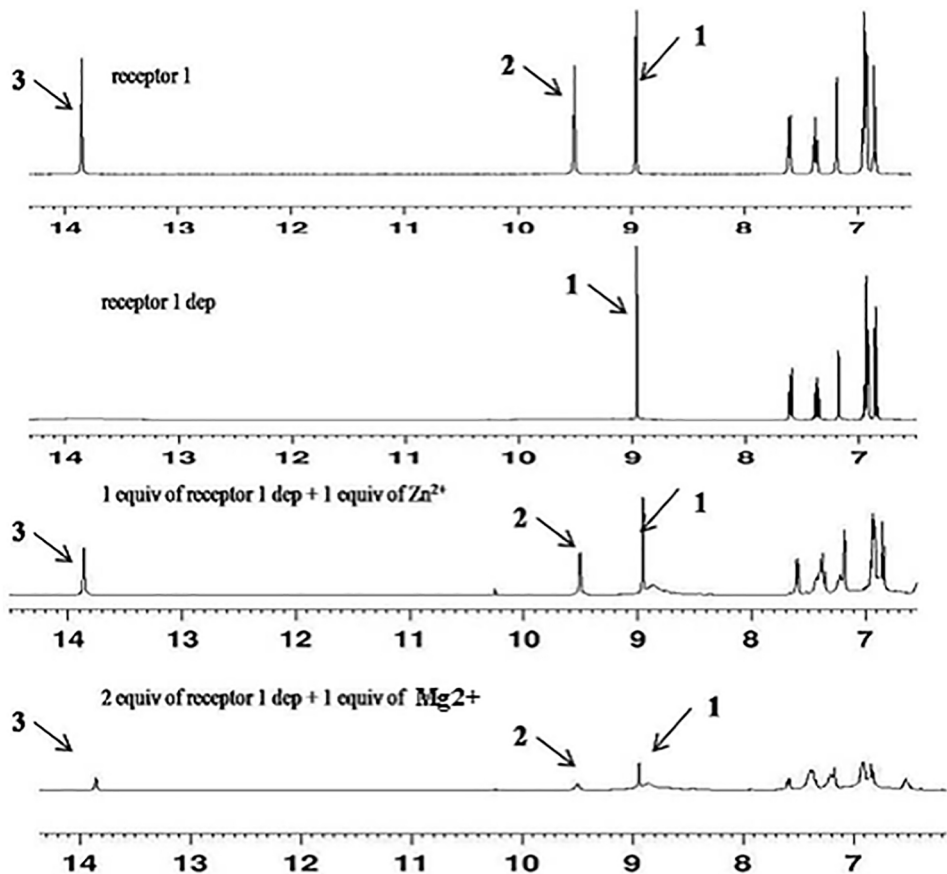


Figure 10

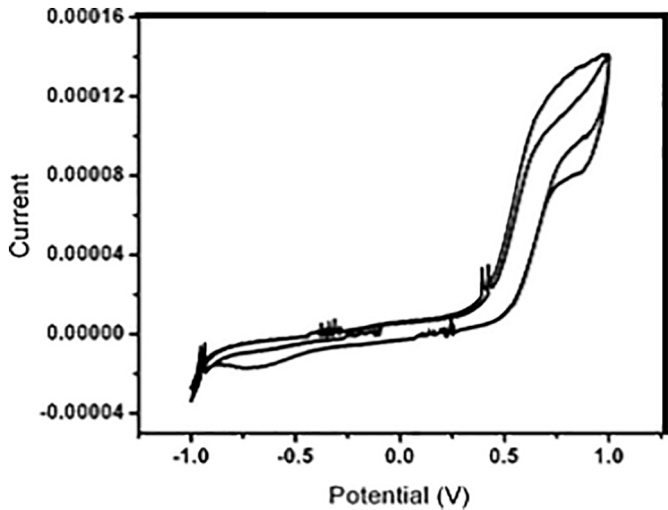


Figure 11

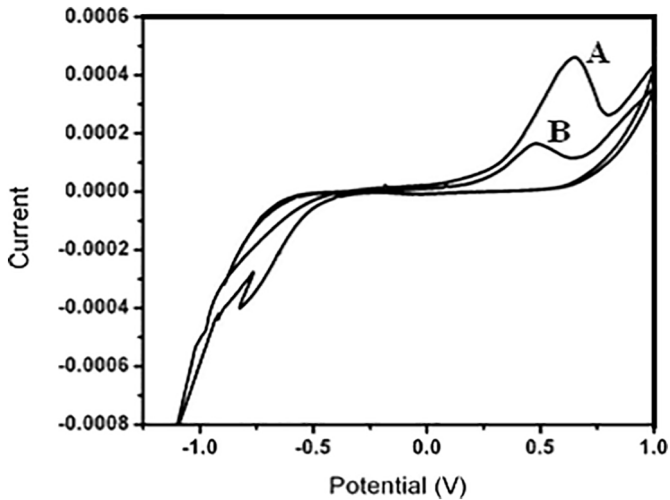


Figure 12

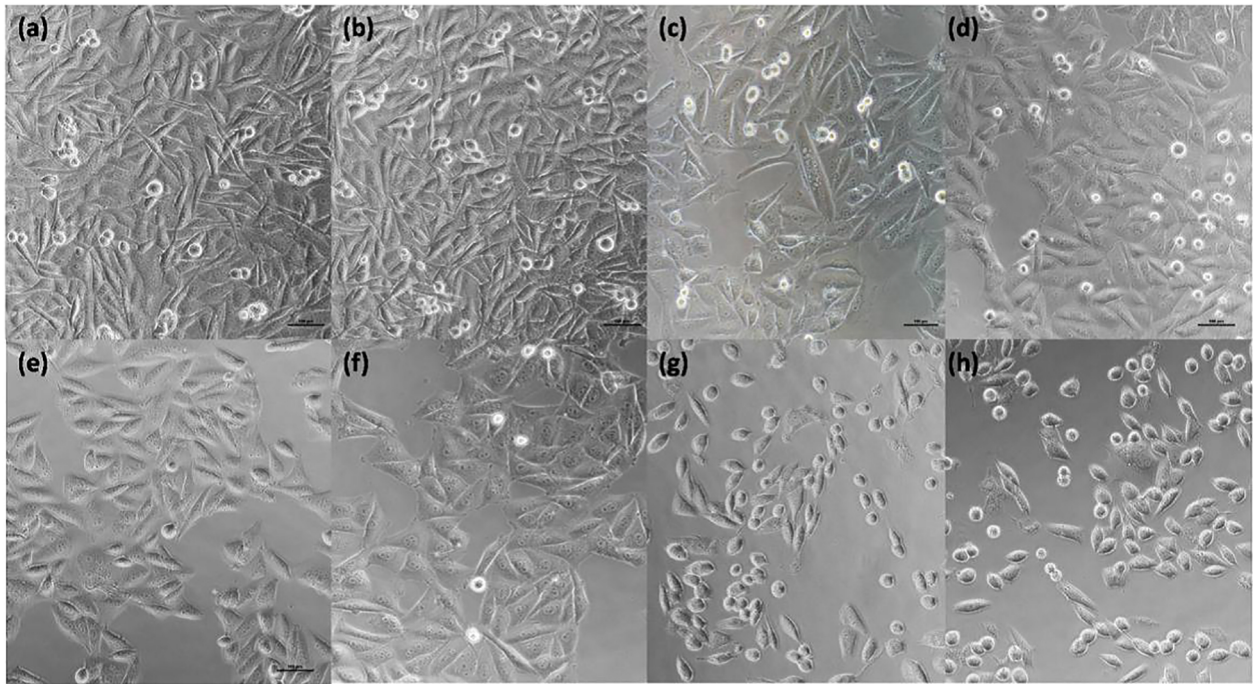


Figure 13

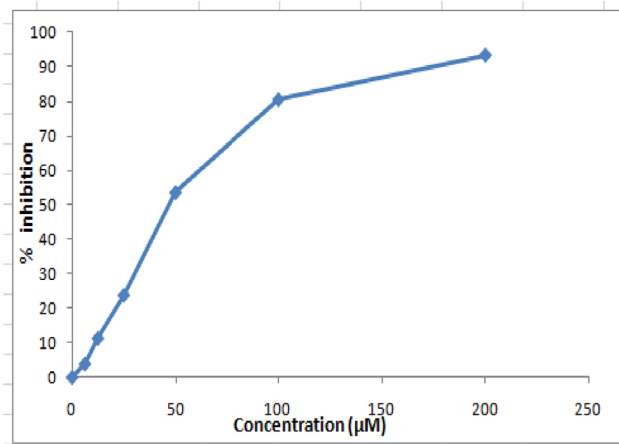
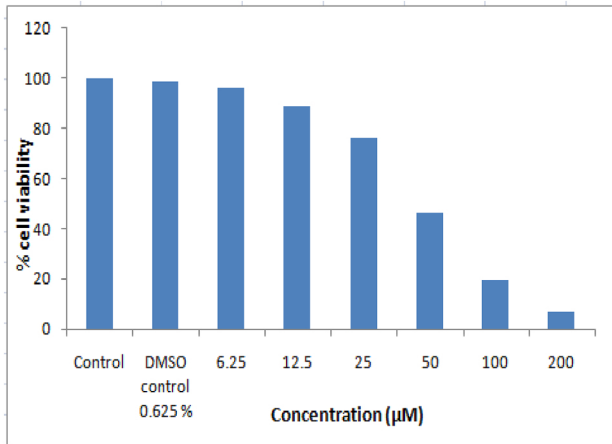


Figure 14

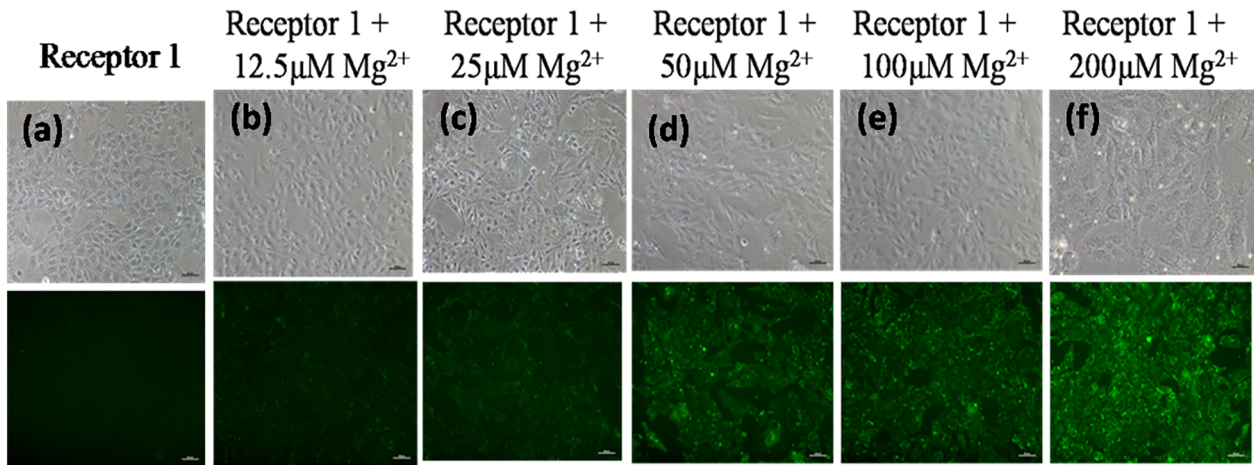


Figure 15

Receptor 1

Receptor 1 +  
 $12.5\mu\text{M}$  of  $\text{Zn}^{2+}$

Receptor 1 +  
 $25\mu\text{M}$  of  $\text{Zn}^{2+}$

Receptor 1 +  
 $50\mu\text{M}$  of  $\text{Zn}^{2+}$

Receptor 1 +  
 $100\mu\text{M}$  of  $\text{Zn}^{2+}$

Receptor 1 +  
 $200\mu\text{M}$  of  $\text{Zn}^{2+}$

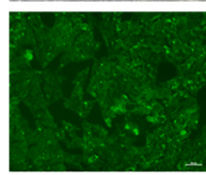
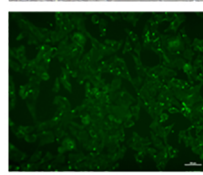
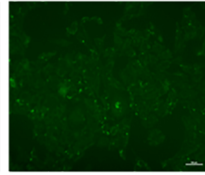
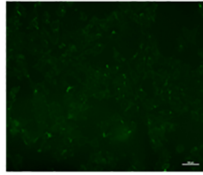
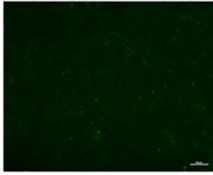
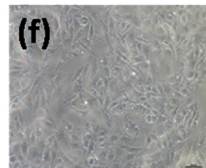
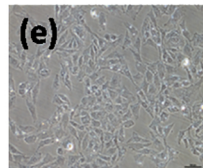
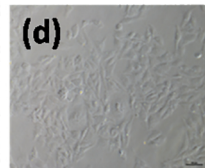
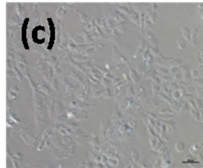
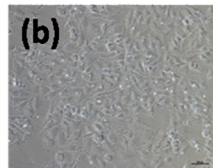
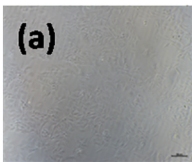


Figure 16

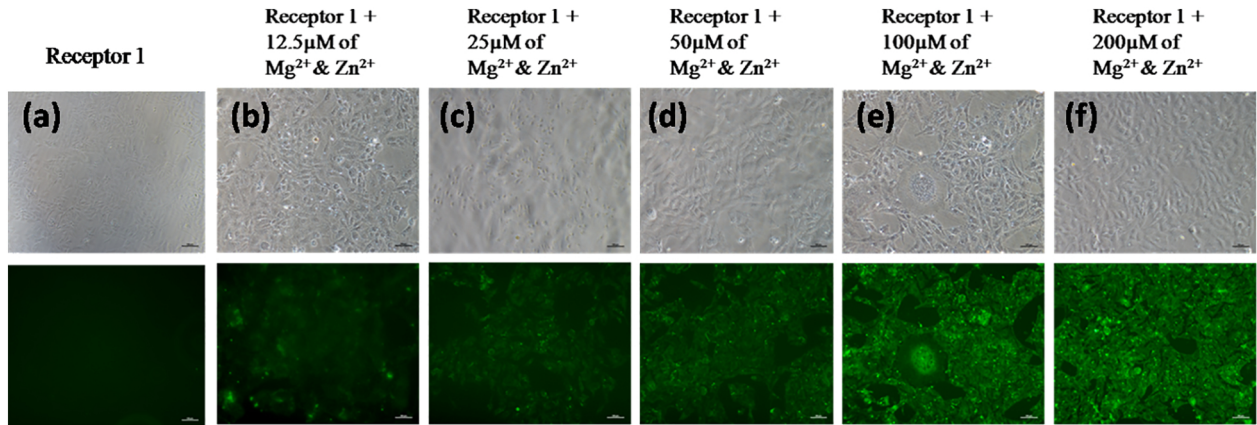


Figure 17

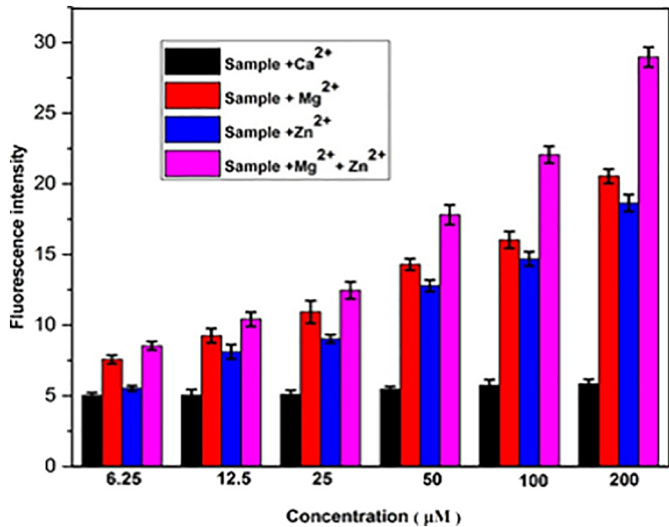


Figure 18